

## HYSTERESIS EFFECTS OF THE NICKEL-BOVINE SERUM ALBUMIN IN SOLUTION

A. IOANID, S. ANTOHE\*

*University of Bucharest, Faculty of Physics, 405 Atomistilor Street, PO Box MG-11, 077125, Magurele-Ilfov, Romania*

For the biological material, the hysteretic effects consist into slow kinetics of their macromolecules following a fast change of the ligand binding. Hysteretic properties defined by a lag in the response of the biomolecule to changes in the ligand level induce the time-depending change of biomolecule function. The kinetics consists from both deformational and orientational dielectric relaxation processes improved by conformational changes of binding protein molecule. In this paper we present any UV-absorbance time-recorded spectra of the nickel-binding BSA for  $[Ni^{2+}] = 3.20 \times 10^{-5} M$  in solution and propose an analysis of the time-depending changes using the usual kinetics-thermodynamics relationship.

(Received October 16, 2013; Accepted November 13, 2013)

*Keywords:* Hysteretic properties, BSA, Rate constant, Dielectric relaxation, Reorganization free energy

### 1. Introduction

Studies of the optical absorption properties are the redutable tools to understanding the electronic properties of the proteins. The changes in observed electronic absorption spectra have been correlated to conformation of the molecular geometry for given conditions, as binding anions/cations ligands, environment, solvent, temperature.

Molecule of the proteins, as stage isolated, or component of biological materials or novel level electronic and optoelectronic molecular devices stage, has a complex structure those fundamental properties are yet partial unknown. On the other hand, the electronic properties of the protein determine hers functions in the biological systems, so that their knowledge may be one key to a large area of future nanotechnology applications in diagnose, treatment and therapeutic drug design/release fields [1]. It is known that the transition metals catalyze various biological processes and their reactivity depends on the nature of the ligands, coordination symmetry and oxidation state of the metal. Proteins as parts of the biological systems, bind the metal ions and form new protein-ion complexes with side-chain terminal groups as ligands heaving kinetic specific properties.

Hysteretic properties defined by a lag in the response of the biomolecule to changes in the ligand level induce the time-depending change of biomolecule function. To study the hysteretic effects of the ion-binding serum albumins as the mainly carrier in vivo, is a major practical interes for biology, medicine and farmacology, so that to complete their benefits, these studies require any multidisciplinary contributions[2]. Serum albumins (both human HSA and bovine BSA) have a variety of binding sites for transition metal ions, as  $Cu^{2+}$ ,  $Ni^{2+}$ ,  $Co^{2+}$ ,  $Cd^{2+}$ ,  $Al^{3+}$  [3], and also for paramagnetic lanthanide ions  $Eu^{3+}$ ,  $Gd^{3+}$  [4]. Insertion by binding of the  $Ni^{2+}$  into active sites of any representative proteins as serum albumins generates the biological systems as nickel-processing systems, with molecular recognition, nickel transport and enzymatic functions.

---

\*Corresponding: [santohe@solid.fizica.unibuc.ro](mailto:santohe@solid.fizica.unibuc.ro)

In vitro studies have been shown that the properties of the nickel-binding proteins are strongly dependent on the metal concentration. The NMR results demonstrate that the probability than  $Ni^{2+}$  binds at N-terminal sites both of HSA and BSA, has a maximum value for  $Ni^{2+}$ /albumin molar ratio of  $\sim 0.8$  for HSA, and  $\sim 1$  for BSA [3]. Few early studies show that the binding of  $Ni^{2+}$  to HSA and BSA is a positive cooperative process and the Hill coefficient (as cooperativity index) is strongly dependent on  $Ni^{2+}$  concentration having a maximum at  $[Ni^{2+}] \sim 5 \times 10^{-5} M$  [5].

In this paper we present any UV-absorbance time-recorded spectra of the nickel-binding BSA for  $[Ni^{2+}] = 3.20 \times 10^{-5} M$  in solution and propose an analysis of the time-depending changes using the usual kinetics-thermodynamics relationship.

## 2. Hysteretic effects of the ligand-binding protein

### 2.1 General considerations

For the biological material, the hysteretic effects consist into slow kinetics of their macromolecules following a fast change of the ligand binding. Experimental results identify any low rate mechanisms for timing behaviour of the ligand-macromolecule complex as the molecule isomerization, polymerization or depolymerization, any changes of the molecule configuration (e.g., unfolding or aggregation). The hysteretic effects that control the rate of the kinetic state change of macromolecule are observed for time intervals greater than that for equilibrium binding process. Both the unfolding and aggregation of proteins consist into conformational changes of molecule, so that the environment of their active sites for a given ligand is changed for both inside and exposure molecule to solvent. Thus, at same ligand concentration, the unfolding may drive the ligand dissociation, while the ligand excess induces diminution of the ligand effect. Rate of the kinetic effects depends on the protein concentration, and is greater for protein concentration below  $10^{-7} M$  and is small above  $10^{-5} M$  [2].

### 2.2 Binding interactions cooperativity

Kinetics is a generic term used to describe both the rates at which processes occur and the field associated with the study of their mechanisms. Binding and dissociation processes will be characterized not only by the equilibrium constants, but also by how fast association/dissociation occur. For the simple case of 1:1 stoichiometry, the equation of the reversible binding process ligand L to protein R as receptor giving RL complexes, is:



And the equilibrium constant for the association/dissociation process  $K_a$ ,  $K_d$  respectively, are defined by:

$$K_a = \frac{[RL]}{[R] \cdot [L]}$$

$$K_d = \frac{1}{K_a} = \frac{[R] \cdot [L]}{[RL]}$$

Where  $[RL]$  is the concentration of formed complexes and  $[R]$ ,  $[L]$  of free protein and ligand, respectively, remaining in solution after binding, at equilibrium.

Binding of ligands has any remarkable effects on BSA stability, inducing any conformational transition of their molecule, that may be associated to a controlled functional unfolding process by a native-denatured (N-D) transition with the equilibrium constant  $K_d = K_{N-D} = \frac{[D]}{[N]}$ ,  $[D]$  and  $[N]$  being the denatured and native protein concentration, respectively.

This constant can then be used to compute a standard free energy of the unfolding process,  $\Delta G_{D-N}^0$  [6,7]. Thus, using relationship between the kinetics and thermodynamics of binding, one may write:

$$\Delta G^0 = -k_B T \ln K_d$$

Experimental results show that the  $K_{N-D}$  of BSA is extremely sensitive to the concentration of high affinity ligands in the aqueous solutions. Thus, an increase in urea concentration from 3.5 to 6 M changes  $K_{N-D}$  by more than 100-fold. This behaviour contrasts with those of other common organic solutes, as glycine and  $\beta$ -alanine, that although increase the dielectric constant of solution, stabilize the native conformation of the protein rather than facilitate denaturation [8].

Biological molecules like BSA are receptors with multiple binding sites for a ligand that are initially equivalent. However, when a ligand binds to one site it induces any changes in the receptor (typically a conformational geometry change) that affect the affinity of the remaining sites for the same ligand to either increase (positive cooperativity then changes in native conformational flexibility are favorable for binding) or decrease (negative cooperativity then the same changes are unfavorable for binding or then first binding induces any loss of freedom for entire molecule). Binding of a second molecule of the same ligand may induce yet another perturbation and so forth [9].

Quantifier of the ligand-receptor binding may be expressed by the fraction of sites filled by binding (or the fraction of ligand complexed), or fractional saturation,  $f_B \in [0,1]$ , defined as ratio of the concentration of ligand bound at protein to the total concentration of binding sites of protein. If a receptor has  $n$  binding sites for the same ligand, the fractional saturation is related to free ligand concentration [L] by the Adair equation [10]:

$$f_B = \frac{K_1[L_1] + 2K_1K_2[L_2][L_1] + \dots + jK_1K_2 \dots K_j[L_1][L_2] \dots [L_j] + \dots + nK_1K_2 \dots K_n[L_1][L_2] \dots [L_n]}{1 + K_1[L_1] + K_1K_2[L_2][L_1] + \dots + K_1K_2 \dots K_j[L_1][L_2] \dots [L_j] + \dots + K_1K_2 \dots K_n[L_1][L_2] \dots [L_n]}$$

Where  $K_j$  is stoichiometric equilibrium constant for the successive stoichiometric step  $j$ . For high positive cooperativity of binding, the concentrations of any intermediate complexes may be neglected in final solution, and  $[L_j] \sim [L_n]$ , and  $[L_n]^n \sim [L]$  is the final free ligand in solution. In this case,  $f_B$  has the expression:

$$f_B = \frac{nK_{a,ef} [L]}{1 + K_{a,ef} [L]}$$

Respectively,

$$\overline{f_B} = \frac{f_B}{n} = \frac{K_{a,ef} [L]}{1 + K_{a,ef} [L]}$$

Where  $\overline{f_B}$  is the fractional saturation per binding site and  $K_{a,ef} \sim K_1K_2 \dots K_n$ , is an *effective* (measurable) ligand-protein association equilibrium constant. Thus, the protein-ligand binding is positively cooperative if the plot of  $f_B$  versus [L] has a characteristic sigmoidal shape and the ratio of successive stoichiometric binding constants is greater than statistical ratio 1:1, namely  $K_j > K_{j-1}$ . New *effective* association equilibrium constant  $K_{a,ef}$  depends of whole binding process because from the above definition, we obtain:

$$K_{a,ef} = \frac{1}{[L]} \frac{\overline{f_B}}{(1 - \overline{f_B})}$$

$K_{a,ef}$  increases then  $\overline{f_B}$  increases and [L] decreases and may be evaluated as  $K_{a,ef} = \frac{1}{K_{d,ef}}$ , where  $K_{d,ef}$  is determined from dissociation kinetics studies. If  $K_{a,ef} \neq K_a$ , then the binding process is

cooperative, and  $K_{a,ef} \sim K_a^h$ , so that if  $h > 1$ , has positive cooperativity, while for  $h < 1$ , has negative cooperativity.

The BSA:Ni<sup>2+</sup> binding process has  $h \approx 2$  for  $[BSA] = 1 \times 10^{-4}M$ , proofing that two sites on protein surface are successive bonded [5].

### 2.3 Kinetics-thermodynamics relationship

Interactions binding ligand to receptor site are specific for each ligand-receptor site pair and the affinity of an active protein site is measured by their free energy of binding  $\Delta G$ . If all the binding sites are independent, then the forces of the first binding process, will affect the affinity of the remainder sites, by one or more of intramolecular interactions: dipole-dipole, dipole-induced dipole, ion-dipole, ion-induced dipole, London interactions, hydrogen-bonding, sulphur-bonding, apolar interactions.

Primary binding ligand to protein via an specific ligand-receptor pair affinity improve any changes both of the local environments of protein bonded sites and molecule exposure to solvent. Thus, the affinity of the global binding process includes other non-specific contributions providing by change of the molecule conformational geometry and consequently, by increasing of their surface exposed to ligand, by change of the molecule dynamics (translational and/or rotational diffusion).

Binding of heavy metal atoms having high affinity for sulphur may disrupt any disulphide (S-S) bonds that results in loss of the BSA bioactivity by the alteration in their tertiary structure.

The metal ions may be considered as redox cofactors for proteins whose binding controle both the intramolecular and intermolecular electron transfer kinetics. A protein molecule complexed by binding their ligands L with metal ions M, may be excited by charge transfer transitions metal to ligand (M-L) (or ligand to metal (L-M)). The electron transfer direction depends on the oxidation state of ion and the transfer rate may be appreciated by the Born-Oppenheimer approximation transition probability written as:

$$k_e = \frac{4\pi^2 H_{ab}^2}{h} e^{-\frac{\Delta G}{k_B T}}$$

Where  $H_{ab}$  is the overlap integral of the donor and acceptor orbital systems,  $\Delta G$  is the activation free energy of transition between the ground state and the low-energy Frank-Condon final state,  $h$  and  $k_B$  are Plank's and Boltzmann's constants respectively, and  $T$  is the temperature [11,12].

Metal ion-protein site binding process consists to an intermolecular electronic transfer, while an intramolecular charge transfer M-L (or L-M) is induced by photoexcitation an optical transition between ground and excited states of the complexed protein site. In this case, the excess electronic energy transfered to nucleic vibrations, followed by whole system configuration fast relaxation. It is known that the initial excitation from the ground state to the higher-lying excited state (by charge-transfer or ligand-field transition) is followed by relaxation to the lowest-energy excited state (Franck-Cordon state) of the system [13].

More experimental and computational results support the linear response approximation [14] for the activation free energy of the electron transfer that consists from the standard free energy  $\Delta G^0$  as the specific affinity of donor/acceptor pair and the reorganization energy  $\lambda$  as energy to attain the equilibrium of whole system.

As configurational change, the reorganization occurs as response to the displacement of the electron charge, so that it is primarily electrostatic in origin. The reorganization consists into a dielectric relaxation process of both the protein molecule and solvent. The average dipole moment  $p_g$  of the protein molecule for ground state is adjusted to new look (in magnification and orientation)  $p_{ex}$  by electronic polarization of the binding sites, displacements of its atomic groups and intramolecular vibrational redistribution. Finally, the local electric field associated to new molecular charge distribution induces any solvent dynamics, via solvatochromism phenomena [15].

In theirs ground and excited electronic state, the protein molecule reacts differently with the solvent, primarily by the changing solvent environments around chromophore excited state.

The large dipole moment associated with the optical transition produces a significant solvation response in simple solvents (e.g., water), measuring by dynamic Stokes shift of the fluorescence emission spectrum [16] or by timing shift of the optical absorbance peak. Thus, after the instantaneously polarization response (electronic polarisation of water molecule), the dynamics of the surrounding water molecules consists to any slow nondiffusive (e.g., local reorientation) motions of orientational polarization, followed by much slower diffusive processes of the new embedded protein molecule.

By both the intramolecular (charge transfer optical transitions) and intermolecular (protein-ion binding, protein-protein interactions) electron transfer, the transition of a single conformational molecule state to an ensemble of random ones is driven by an increasing of the entropy, so that the activation free energy is  $\Delta G = \Delta G^0 + \lambda$ , where  $\lambda$  is the reorganization free energy that is determined by dielectric response to charge transfer [17].

Taking into account the above considerations, the total free energy of binding  $\Delta G$  may be culled from many contributions that may be grouped in least three categories:

$$\Delta G = \Delta G_{intrinsic} + \Delta G_{statistical} + \Delta G_{interaction}$$

Where  $\Delta G_{intrinsic} = \Delta G^0$  is the contribution of the specific binding of a ligand to an isolated site,  $\Delta G_{statistical}$  is the contribution due to the change of the specific affinity of site via cooperative binding, and  $\Delta G_{interaction}$  is the contribution due to the new interactions after binding process. On the other hand, the experimental data give:

$$\Delta G = -k_B T \ln K_{exp}$$

So that, it may write:

$$K_{exp} = K_{intrinsic} \cdot K_{statistical} \cdot e^{-\frac{\Delta G_{interaction}}{k_B T}}$$

### 3. Experimental

#### 3.1 Samples and Methods

We present an analysis of the time-recording UV-absorbance spectra of the  $[BSA:Ni^{2+}][1:1]M$  system in phosphate buffer solution for  $(200 \div 350)nm$  spectral range. Spectra were recorded for  $[Ni^{2+}] = 0.32 \times 10^{-4}M$  and  $[Ni^{2+}] = 1.00 \times 10^{-4}M$  in the  $(0 \div 300) min$  range, with first spectrum at  $t = 0 min$ .

BSA with electrophoretic purity were purchased from Sigma Laboratories and as  $Ni^{2+}$  ligands were used nickel chlorate p.a. ( $NiCl_2$ ) from Reactivul Laboratories, Romania.

All samples were prepared with the phosphate buffer solutions containing 8 g NaCl, 0.2g KCl, 1.44 g  $Na_2HPO_4$ , 0.24g  $KH_2PO_4$  and distilled water for  $1000cm^3$  solution. The pH-value has been adjusted to  $(7 \div 7.4)$  with NaOH 0.1M solution. BSA (66.430 mg) and  $NiCl_2$  (0.130 mg) was been dissolved in  $10 cm^3$  of phosphate buffer solution for  $1 \times 10^{-4}M$   $[BSA:Ni^{2+}][1:1]M$  sample. Solutions with any decreasing concentration were obtained by the controllable successive dilution.

All the difference absorbance spectra between  $(BSA:Ni^{2+})[1:1]M$  sample cell and BSA with same concentration reference cell, were recorded using a Perkin Elmer Lambda 35 Spectrofotometer in  $(190 \div 1100)nm$  spectral range. All samples were characterized at room temperature and pressure conditions.

#### 3.2 Time-recording UV-absorbance spectra

The Fig.1 shows the changes appearing in successive UV-absorbance spectra long time ( $\sim 300$  minutes) after the first exposure for the  $0.320 \times 10^{-4}$   $[BSA:Ni^{2+}][1:1]M$  sample.

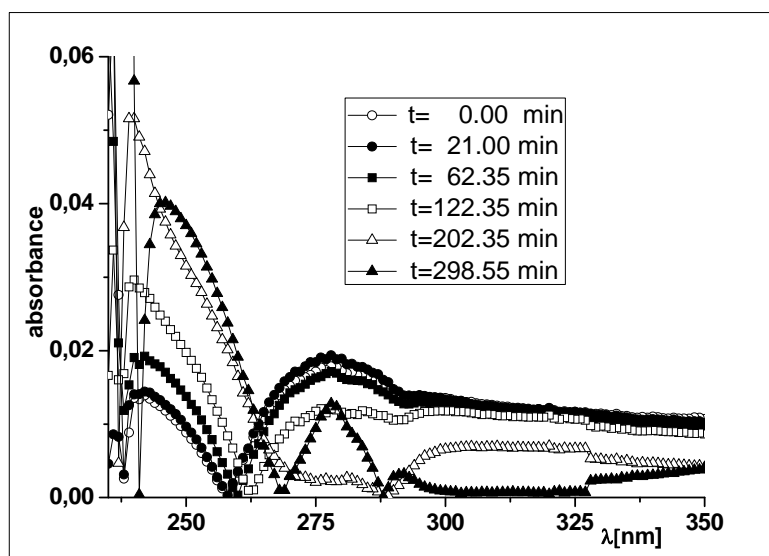


Fig.1. Time dependence of the UV-absorbance spectrum of the  $0.320 \times 10^{-4}$  [BSA: $\text{Ni}^{2+}$ ][1:1]M sample.

First spectrum ( $t = 0$  min) shows two absorption peaks: i) one symmetric large peak at  $\lambda = 280$  nm and another asymmetric on long wavelength side at  $\lambda \approx 236$  nm; ii) for the successive spectra, the  $A_{280}$  absorbance decreases and late after the first spectrum remains symmetric but narrow and preserves spectral position at  $\lambda = 280$  nm, while the  $A_{250}$  absorbance increases, enlarges and their asymmetry extends with shoulder to long wavelength side, Fig.2; after long time ( $\sim 300$  min) the absorbance increases to 2-3 times initial value ( $t = 0$  min) and the peak position shifts to  $\lambda \approx 250$  nm.

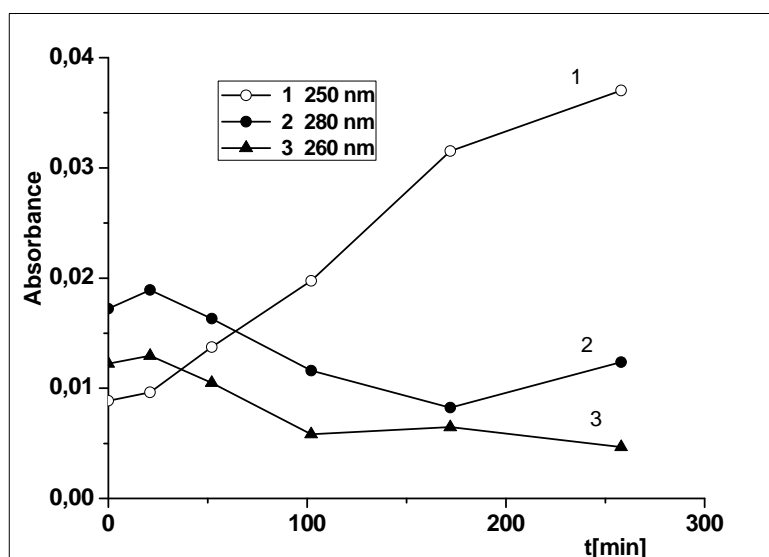


Fig.2. Time dependence of the  $A_{250}$ ,  $A_{260}$ ,  $A_{280}$  absorbances of the  $0.320 \times 10^{-4}$  [BSA: $\text{Ni}^{2+}$ ][1:1]M sample

#### 4. Discussions

Structure of the first absorbance spectrum shows mainly any optical transitions between electronic states of the complexed BSA-Ni<sup>2+</sup> molecule [18]. All the A<sub>250</sub>, A<sub>266</sub>, A<sub>280</sub> absorbance peaks are superimposed to the same intrinsic absorbances of the free BSA molecule. Thus, the absorbance peak A<sub>280</sub> is attributed to delocalized electrons transitions of the aromatic amino-acids tryptophane (Trp) and tyrosine (Tyr) whose absorbance intensity depends on the polar/nonpolar environment of their chromophores, so that the Trp and Tyr residues exposed to solvent and those from inside of protein molecule will absorb differently. Consequently, a conformational protein change that induces a ratio of exposed to solvent/inside protein residues change, may be associated to a decrease in absorbance intensity. The phenylalanine (Phe) residues absorption determines the fine structure of spectrum in  $\lambda \in (250 \div 260) \text{ nm}$  range, while the near UV-band at  $\lambda \approx 260 \text{ nm}$  is attributed to the S-S bonds between cysteine (Cys) residues-pairs that stabilize the folded phase of BSA [19]. On the other hand, the wavelength  $\lambda \approx 236 \text{ nm}$  is the long wavelength limit of the absorbance peak attributed to  $\pi \rightarrow \pi^*$  electronic transitions of the amide groups [20] of BSA molecule. Thus, the absorbance spectrum is very sensitive to conformational change of protein molecule by ligand-binding protein interactions. Therefore, the observed large scale time dependence of the absorbance spectrum may be associated to slow protein molecule configurational changes.

##### *A<sub>280</sub> absorbance peak*

Timing-decrease of the A<sub>280</sub> absorbance peak intensity from Fig.2 may be associated to any changes of the intrinsic chromophores absorbance as Trp, Tyr and S-S bonds in successive new molecular configurations. Ground state dipole moment of the hydrophobic residue Trp is very small, while the electronic excited state has a large dipole moment and the spectral modifications underline a relaxation signature of the solvent molecules around this new large dipole. Particularly, the fast relaxation of the water molecules close to vicinity of the grand dipole moment of the excited Trp residue induces a local solvent rigidity dynamics, so that this new water environment increases the distance between two Trp residues and the A<sub>280</sub> absorbance intensity decreases [21]. The lineshape of the A<sub>280</sub> absorbance peak is thereabout Lorentzian showing that this transition is the same for all protein molecules (both original and deformed) [22]. The A<sub>280</sub> absorbance peak is symmetric and has no Stokes shift showing that the protein molecule deformation is a non-cooperative process [15], while the time depending homogeneous broadening reflects the existence of a continuous set of vibrational sublevels in each electronic state that relax slow for time [23]. On the other hand, the Ni<sup>2+</sup> binding implying very probable the histidine (Hys) residue from a shorter S-S loop [18, 25] induces a cleavage of the S-S bonds system that change the protein molecule conformation to one whose chromophore residues (Trp,Tyr,Phe) resides at sites significantly exposed to solvent. Assuming the conformational molecule change to a first-order kinetics transition process, their rate may be write:

$$\frac{dc_{new}}{dt} = k_{280}(c_0 - c_{new})$$

$$\frac{dc_{new}}{(c_{new} - c_0)} = -k_{280}dt$$

Where  $k_{280}$  is the rate constant,  $c_{new}$  and  $c_0$  are the molar concentration of the deformed and original protein molecule structure, respectively. Accomodating to the Beer-Lambert law and using the A<sub>280</sub> absorbance values from Fig.2, after integration one obtain:

$$\ln \frac{A_{280}(t)}{A_{280}^0} = -k_{280}t$$

Where  $A_{280}^0$  is of first ( $t = 0$ ) spectrum value. Thus, the  $k_{280} = 9.363 \times 10^{-5} \text{ s}^{-1}$  value is obtained by the linear fit shown in Fig.3.

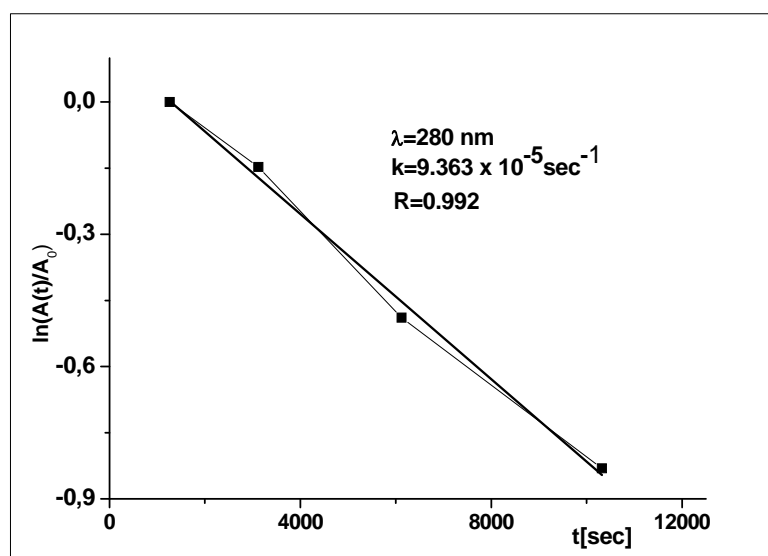


Fig.3. Determination of the rate constant of the conformational change process,  $k_{280}$

The thermodynamic parameters of the protein deformational transition may be calculated with the transition-state theory, so that the equilibrium constant  $K_{280}$  is:

$$K_{280} = k_{280} \frac{h}{k_B T}$$

and the free energy of the transition process is:

$$\Delta G_{280} = -RT \ln K_{280} = -RT \ln \left( \frac{k_{280} h}{k_B T} \right)$$

Where  $R$  is the universal gas constant. We obtain  $K_{280} = 9.025 \times 10^6 \text{ mol}^{-1}$ .

#### **$A_{250}$ absorbance peak**

Contrast with the  $A_{280}$  absorbance peak, the lineshape of the  $A_{250}$  absorbance peak is thereabout a Gaussian adequated to inhomogenous system statistical distributions [22]. In this case, we consider the all sorts of oscillators states distribution, both of complexed and free molecules. This absorbance peak is attributed to a charge transfer transition beetwen from ground to photoexcited electronic states of the BSA-Ni<sup>2+</sup> complex [18].

The interaction between complexed and free protein molecule dipoles induces the peak position shift, while the red side broading may be attributed to an inhomogenous statistical distribution of the electronic transition energies of the side-chain amides of new complexed protein molecule-solvent dipoles configurations [23].

Taking into account the above considerations, the timing-increase of the  $A_{250}$  absorbance peak intensity from Fig.2 may be associated to an increase of the complexed molecule concentration, via the positive cooperative binding process favorised by molecule deformation. In this case,  $c_{new}$  and  $c_0$  is the current molar concentration of the complexed, and free protein respectively. The rate of the evolution to the equilibrium ( $c_{new}(t \rightarrow \infty)$ ) may be write:

$$\frac{dc_{new}}{dt} = k_{250}(c_0 - c_{new})$$

Where  $k_{250}$  is the rate constant that is determined from the linear fit shown in Fig.4 of the equation:

$$\ln \frac{A_{250}(t)}{A_{250}^0} = -k_{250}t$$

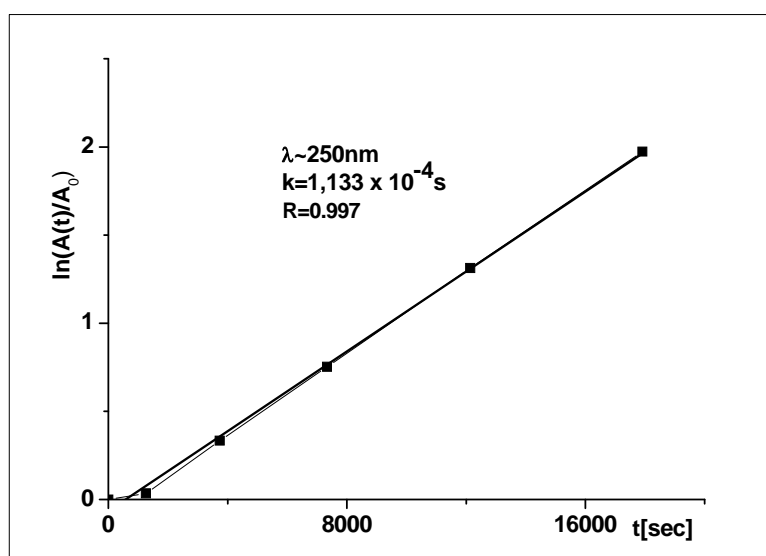


Fig.3. Determination of the rate constant of the conformational complexed molecule dynamics,  $k_{250}$ .

Using the absorbance values from Fig.2. we obtain the rate constant  $k_{250} = 1.133 \times 10^{-4} \text{ s}^{-1}$ , and via the same above way, the equilibrium constant  $K_{250} = 1.177 \times 10^7 \text{ mol}^{-1}$ . Then the free energy of the protein complexation evolution is:

$$\Delta G_{250} = -RT \ln K_{250} = -RT \ln \left( \frac{k_{250} h}{k_B T} \right)$$

The notable result  $k_{250} \gg k_{280}$  shows that the protein molecule complexation process by  $\text{Ni}^{2+}$  binding is more than 1:1 versus the conformational protein molecule change and proofs the positive cooperativity of the binding process [18].

Finally, we calculate:

$$\frac{K_{280}}{K_{250}} = \frac{K_{intrinsic}^{280}}{K_{intrinsic}^{250}} \cdot \frac{K_{statistical}^{280}}{K_{statistical}^{250}} \cdot e^{-\frac{\Delta G_{interaction}^{280} - \Delta G_{interaction}^{250}}{k_B T}}$$

Taking into account the above considerations, the pair specific affinity is the same for both  $A_{280}, A_{250}$  absorbances and  $K_{intrinsic}^{280} \approx K_{intrinsic}^{250}$ , while  $K_{statistical}^{280} \neq K_{statistical}^{250}$  and  $\frac{K_{statistical}^{280}}{K_{statistical}^{250}} < 1$  (e.g., 0.5 for BSA- $\text{Ni}^{2+}$  [5]), because the processes differ by cooperativity. If we consider that the new interactions of deformed and complexated protein molecule are different, then  $\Delta G_{interaction}^{280} \neq \Delta G_{interaction}^{250}$ . Using the  $K_{280}$  and  $K_{250}$  experimental values, we obtain equation:

$$0.383 = e^{-\frac{\Delta G_{interaction}^{250} - \Delta G_{interaction}^{280}}{k_B T}}$$

With solution:

$$\Delta \Delta G = \Delta G_{interaction}^{250} - \Delta G_{interaction}^{280} = \ln 0.383 \times k_B T = -0.959 \times k_B T$$

As result,  $\Delta G_{interaction}^{250} < \Delta G_{interaction}^{280}$ , and because generally  $\Delta G = \Delta H - T\Delta S$ ,  $(\Delta H_{interaction}^{250} - T\Delta S_{interaction}^{250}) < (\Delta H_{interaction}^{280} - T\Delta S_{interaction}^{280})$ . For isothermal conditions, it is reasonable to consider  $\Delta H_{interaction}^{250} \approx \Delta H_{interaction}^{280}$ , so that one obtain  $\Delta S_{interaction}^{250} > \Delta S_{interaction}^{280}$ , namely  $\Delta \Delta S = (\Delta S_{interaction}^{250} - \Delta S_{interaction}^{280}) = 0.959 \times k_B$ . Each of two terms represents the configurational entropy contribution,  $(\Delta S_{interaction}^{250})$  due to the complexated BSA- $\text{Ni}^{2+}$  molecule, and  $\Delta S_{interaction}^{280}$  due to deformed free BSA molecule kinetics. This inequality exprimes that the timing evolution of the electronic excited state of complexed BSA molecule consists into more conformations, so that the configurational entropy of

system increases. Moreover,  $\Delta\Delta S > 0.693 \times k_B$  that is the maximum value of the configurational entropy of two non-interacting components disordered system, so that it is realistic to consider the reorganization of all free deformed and complexed BSA molecules, solvent dipoles, via non-specific (dielectric) interactions as dipole-dipole (for both complexed protein molecules and solvent dipoles system), protein dipole-solvent polarizability, protein polarizability-solvent dipole, protein polarizability-solvent polarizability, rather than by specific interactions as the hydrogen bonding.

The kinetic processes following to photoexcitation of complexed protein molecules are very slow, with long relaxation time  $\tau_{relax} \sim \frac{1}{k} \sim 10^5 \div 10^6 s$ ,  $k = k_{280}, k_{250}$ , out of the range of the resonant dielectric response (electronic and vibrational polarizability), but  $\tau_{relax} \sim \tau_{diel}$  for the low frequency dielectric relaxation processes. Moreover,  $\tau_{relax}$  is still more of the chemical binding process  $\tau_{chem}$ , so that the both transversal and rotational diffusional dynamics components play an important role. It is known that the mean value of the diffusion coefficient  $D$  depends of the free ligand fraction  $\alpha$  in solution, namely [24]:

$$\langle D(t) \rangle = \alpha D^{free} + (1 - \alpha) D^{bond}$$

So that finally, the measured value of  $D$  is determined by bonded (complexed) molecule contribution  $D^{bond}$ . On the other hand,  $D$  depends on the protein molecule geometry by the Stokes-Einstein-Debye equation [26], so that, for an ellipsoidal geometry,

$$D = \frac{k_B T}{6\eta V g_i}$$

Where  $g_i$  is the Perrin factor and depends only on the axial ratio  $p = \frac{a}{b}$  of the ellipsoid. The native BSA molecule in solution has a prolate ellipsoidal shape with  $p = 2.1$  [27], but the stability of BSA molecule complexed by  $Ni^{2+}$  ions binding imposes the deformation its structure from compact to one elongated, so that, for prolate ellipsoid form with  $p = 3.5$ ,  $g_i \approx 2.9$  [26], and the new conformational complexed molecule diffuse more slow than free.

#### 4. Conclusions

Slow kinetics of the complexed protein molecule in solution observed from the time dependence of the electronic absorbance spectra is mainly determined on its conformational change. The deformation of the molecular structure from compact to one elongated consists to an exposure increasing of their hydrophobic residues. The large transition dipole moment that results from the migration of electric charges during an electronic transition by photoexcitation induces a reorganization of the surrounding solvent dipoles via four major dielectric interactions: dipole-dipole (for both complexed protein molecules and solvent dipoles system), protein dipole-solvent polarizability, protein polarizability-solvent dipole, protein polarizability-solvent polarizability, rather than by specific interactions as the hydrogen bonding. Thus, the new fixed solvation shell surrounding the complexed protein molecule by the above hydrophobic interactions, improves to which a very slow kinetics. It is expected that for the same protein, the slow kinetic processes are controlled by both the ligand and solvent properties.

#### References

- [1] Philippe Rondeau, Giovanna Navarra, Valeria Militello, and Emmanuel Bourdon, Protein aggregation, Chap.5, pp 1-22, ISBN 978-61761-815-4, 2010 Nova Publishers, Inc., Ed. Douglas A. Stein, email: [rophil@univ-reunion.fr](mailto:rophil@univ-reunion.fr).
- [2] Carl Frieden, Kinetics Aspects of regulation of Metabolic Processes, The Journal of Biological Chemistry, **245**(21), 5788 (1970).
- [3] Peter J. Sadler, Alan Tucker and John H. Viles, J. Biochem. **220**, 193 (1994).
- [4] Thomas J Meade, Alisha K. Taylor and Steven R Bull, Current Opinion in Neurobiology **13**, 597 (2003).

- [5] Zhou Yongoia, Hu Xuing, Ouyang Di, Huang Jiessheng, Wang yumen, *Biochem. J.* **304**, 23 (1994).
- [6] A.Szilagyı, J.Kardos, L.Barna, P.Zavodschi, 10 Protein folding, Springer-Verlag Berlin Heidelberg pag 16, 2007.
- [7] Connie M. Chung, Jenny D. Chiu, Laureen H. Connors, Olga Gursky, Amareth Lim, Andrew B. Dykstra, Juris Liepnieks, Merrill de Benson, Catherine E. Costello, Martha Skinner, and Mary T. Wals, Thermodynamic Stability of a kI Immunoglobulin Light Chain: Relevance to Multiple Myeloma, *Biophysical Journal* **88**, 4232 (2005).
- [8] Irvin M.Klotz, Equilibrium constants and free energies in unfolding of proteins in urea solutions, *Proc.Natl. Acad. Sci. USA*, **93**, 14411 (1996).
- [9] <http://www.123people.com/s/charles+r+sanders>
- [10] I.M.Klotz, *Proc.Natl.Acad.Sci.USA*, **90**, 7191 (1993).
- [11] Kim A. Sharp, Calculation of Electron Transfer Reorganization Energies Using the Finite Difference Poisson-Boltzmann Model, *Biophysical Journal*, **73**, 1241 (1998).
- [12] William B.Davis, Michael R. Wasielewski, and Mark A. Ratner, Vladimiro Mujica, Abraham Nityan, Electron Transfer Rates in Bridged Molecular SzstemŞ A Phenomenological Approach to relaxation, *J. Phzs. Chem. A*, **101**, 6158 (1997).
- [13] James K. Mccusker, Femtosecond Absorption spectroscopy of Transition Metal aCharge-transfer Complexes, *Acc. Chem. Res.*, **36**, 876 (2003).
- [14] Marcus,R.,and N.Sutin, Electrons transfers in chemistry and biology, *Biophys.Acta*, **811**, 265 (1985).
- [15] Megan H.J.Oh, Mayrose R. Salvador, Cathy Y. Wong, and Gregory D. Scholes, Three-Pulse Photo-Echo Peak Shift Spectroscopy and Its Application for the Study of Solvation and Nanoscale Excitons, *ChemPhys Chem*, **12**, 88 (2011).
- [16] William Childs and Steven G. Boxer, Solvation Response along the Reaction Coordinate in the Active Site of Ketosteroid Isomerase, *J.Am.Chem.Soc.*, **132**, 6474 (2010).
- [17] Edward L. Mertz, and Lev I. Krishtalik, Low response in enzyme active site, *PNAS*, **97**(5), 2081 (2000).
- [18] M.Dieaconu, A.Ioanid, S.Iftimie, and S.Antohe, *Digest Journal of Nanomaterials and Biostructures*, **7**(3), 1673 (2012).
- [19] Franz-Xaver Schmid, *Biological Macromolecules:UV-visible Spectrophotometry*, *Encyclopedia Of Life Sciences*, 2001, [www.els.net](http://www.els.net).
- [20] Bhavya Sharma and sanford A. Asher, *J. Phys. Chem. B*, **114**, 6661 (2010).
- [21] Samir Kumar Pal, Jorge Peon, Ahmed H. Zewail, *PNAS*, **99**(4), 1763 (2002).
- [22] S.M.Vlaming, V.A. Malyshev, J.Knoester, *Phys Rev.* **B79**, 205121 (2009).
- [23] Thomas Simonson, Gaussian fluctuations and linear response in an electron transfer protein, *PNAS*, **99**(10), 6544 (2002).
- [24] Bernard Valer, *Molecular Fluorescence: Principles and Applications*, Wiley-VCH Verlag GmbH, p.67, 2001.
- [25] Mark Klewpatinond and John H.Viles, Fragment length influences affinity for Cu<sup>2+</sup> and Ni<sup>2+</sup> binding to His<sup>96</sup> or His<sup>111</sup> of the prion protein and spectroscopic evidence for a multiple histidine binding only at low pH, *Biochem.J.*, **404**, 393 (2007).
- [26] M.Luisa Ferrer, Ricardo Duchowicz, Beatriz Carrasco, Jose Garcia de la Torre, A. Ulises Acuna, *Biophysical Journal* **80**, 2422 (2001).
- [27] Amit Das, R. Chitra, R.R. Choudhury, M.Ramanadham, Structural changes during the unfolding of Bovine Serum Albumin in the presence of ureea: A small-angle neutron scattering study, *Pramana-J.Phys.*, **63**(2), 363 (2004).